26

Mobile Robotic Systems

26.1 Introduction
26.2 Fundamental Issues
Definition of a Mobile Robot • Stanford Cart • Intelligent Vehicle for Lunar/Martian Robotic Missions • Mobile Robots — Nonholonomic Systems
26.3 Dynamics of Mobile Robots
26.4 Control of Mobile Robots

Nenad M. Kircanski
University of Toronto

26.1 Introduction

This subsection is devoted to modeling and control of mobile robotic systems. Because a mobile robot can be used for exploration of unknown environments due to its partial or complete autonomy is of fundamental importance. It can be equipped with one or more manipulators for performing mission-specific operations. Thus, mobile robots are very attractive engineering systems, not only because of many interesting theoretical aspects concerning intelligent behavior and autonomy, but also because of applicability in many human activities. Attractiveness from the theoretical point of view is evident because no firm fundamental theory covering intelligent control independent of human assistance exists. Also, because wheeled or tracked mobile robots are nonholonomic mechanical systems, they are attractive for nonlinear control and modeling research. In Section 26.2 of this chapter, fundamental issues are explained regarding nonholonomic systems and how they differ from holonomic ones. Although we will focus attention mostly on wheeled mobile robots, those equipped with tracks and those that rely on legged locomotion systems are addressed as well. The term "mobility" is addressed from the standpoint of wheeled and tracked platform geometry. Examples provided are also showing how different platforms have been built in practice.

Section 26.3 covers dynamics of mobile robots. Models range from very complex ones that include dynamics of deformable bodies to relatively simple models mostly used to facilitate development of control algorithms. The discussion concludes with some model transformations that help obtain relatively simple models.

The next section is devoted to control issues from the standpoint of both linear and nonlinear control theories. We explain the difference between controllability in the linear system theory and controllability of mobile robots, having in mind that a mobile robot is a nonlinear system.

26.2 Fundamental Issues

26.2.1 Definition of a Mobile Robot

A definition of a mobile robotic system does not exist. The International Standards Organization (ISO), has defined an industrial robot as:

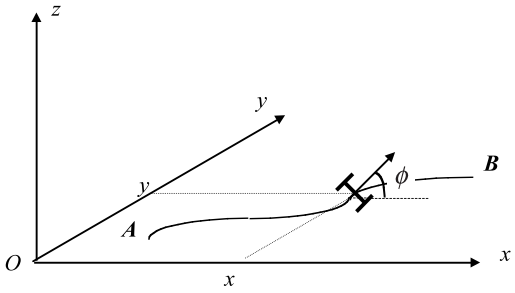

FIGURE 26.1 Definition of coordinates.

Definition 1: An *industrial robot* is an automatic, servo-controlled, freely programmable, multipurpose *manipulator*, with several axes, for the handling of workpieces, tools, or special devices. Variably programmed operation make possible the execution of a multiplicity of tasks.

This definition clearly indicates that the term "industrial robot" is linked to a "manipulator," meaning that such a mechanical system is attached to a base. Typically, the base is fixed with respect to a ground or single-degree-of-freedom platform mounted on rails. We also observe that an industrial robot must have a programmable control system so that the same robot can be used for different tasks.

A mobile robot has two essential features that are not covered by this definition. The first is obviously mobility, and the second is autonomy. A minimum requirement for a mobile robot is to be capable of traversing over flat horizontal surfaces. Given a point $\boldsymbol{A}$ on such a surface S, where the robot is positioned at a time instant t, the mobile robot must be capable of reaching any other point $\boldsymbol{B}$ at a certain distance $d < \infty$ from $\boldsymbol{A}$, in a finite time T. Here, we should clarify the meaning of the term "position." Let us assume that a coordinate frame $Oxyz$ is attached to the surface so that O belongs to the surface, while the z-axis is normal to the surface (Figure 26.1). Clearly, the position of any point on the surface is defined by coordinates (x, y). But, the position of the robot is actually defined by the coordinates (x, y, ϕ), where ϕ defines the orientation of the chassis with respect to the x axis. Of course the orientation can be defined in many different ways (for example, with respect to y or any other axis in the plane surface). So, mobility means that the robot is capable of traversing from the position (x_A, y_A, ϕ_A) to (x_B, y_B, ϕ_B) in a finite time interval T.

Mobility, as discussed above, is limited in terms of the system's ability to traverse different surfaces. The simplest case is a flat horizontal surface z = constant. Most 4-wheel mobile robots are designed for such terrains. In the case of a smooth surface $z = f(x, y)$, where f is an arbitrary continuous function of x and y, the ability of a wheeled robot to reach any desired point $\boldsymbol{B}$ from a point $\boldsymbol{A}$ on the surface depends upon (1) the ability of the robot to produce enough driving force to compensate for gravity force while moving toward the goal point; and (2) the presence of sufficient friction forces between the wheels and the ground to prevent continuous slippage. Notice also that there is no uniquely defined path between the points $\boldsymbol{A}$ and $\boldsymbol{B}$, and the robot may be incapable of traversing some trajectories, but still capable of reaching point $\boldsymbol{B}$ provided the trajectory is conveniently selected.

In discussions related to mobility a fundamental question concerns climbing and descending stairs, over-crossing channels, etc. Previously we have implicitly assumed that the function f is differentiable with respect to x and y. If this does not hold, as is true for a staircase, mobility can be achieved with tracks or legs. Robots with legs are called "legged-locomotion robots." Such robots are rarely used in practice due to the complexity (and thus reliability and cost) of the locomotion subsystem. Tracked robots are usually six-wheel robots with a set of two tracks mounted on three wheels on the left and three wheels on the right side of the chassis. Each track has a tread

that engages with the edge of the first stair of a staircase. Such engagement allows for lifting the front side of the chassis while the back side remains on the ground. In this phase of climbing, the vehicle tilts backward while moving forward and finally reaches an inclination angle equal to that of the staircase. The tread on the tracks engages with several stairs simultaneously, allowing the robot to move forward.

In the second part of this section, the mobility will be highlighted from the standpoint of nonholonomic constraints. We explain why a manipulator is a holonomic and why a mobile robot is a nonholonomic system. Prior to that, though, we attempt to define a mobile robot. As mentioned at the beginning of this section, the second essential feature of a mobile robot is autonomy. We know that vehicles have been used as a means of transportation for centuries, but vehicles were never referred to as "mobile robots" before, because the fundamental feature of a robot is to perform a task without human assistance. In an industrial, well-structured environment it is not difficult to program a robot manipulator to perform a task. On the other hand, the term "mobile robot" does not necessarily correlate to an industrial environment, but a natural or urban environment. Industrial mobile robots are called automatic guided vehicles (AGVs). AGVs are mobile platforms typically guided by an electromagnetic source (a set of wires) placed permanently under the floor cover. Tracking of the guidelines is realized through a simple feedback/feedforward control. Thus, an AGV is not referred to as a mobile robot because it is not an autonomous system.

An autonomous system must be capable of performing a task without human assistance and without relying on an electronic guidance system. It must have sensors to identify environmental changes, and it must incorporate planning and navigation features to accomplish a task. More details about these features are given in later sections, but now we provide an example of a simple mobile robot currently used in urban environments: a vacuum-cleaning mobile robot. Such commercially available robots have an ultrasonic-based range-finder mounted on a pan-and-tilt unit. This unit is located on the front end of the chassis and constantly rotates left-and-right and up-and-down independently of the speed of the vehicle. The range-finder is an ultrasonic transceiver/receiver sensor mounted on the unit end-point. The echoes are processed by an on-board computer to identify obstacles around the robot. A planner is a software module that describes the "desired path" so that cleaning is performed uniformly all over the floor surface. The navigator is the software module that provides changes in desired trajectories in accordance with the obstacles/walls located by the sensorial system. Such a robot will automatically slow down and avoid a collision should another vehicle or a human traverse its trajectory. Clearly, autonomy is not necessarily correlated to artificial intelligence. "Intelligent control" can be a feature of a mobile robot, but it is not a must in practice.

Based on the previous discussion we can define a mobile robot as follows:

Definition 2: A *mobile robot* is an autonomous system capable of traversing a terrain with natural or artificial obstacles. Its chassis is equipped with wheels/tracks or legs, and, possibly, a manipulator setup mounted on the chassis for handling of work pieces, tools, or special devices. Various preplanned operations are executed based on a preprogrammed navigation strategy taking into account the current status of the environment.

Although this is not an official definition proposed by ISO, it contains all the essential features of a mobile robot. According to this definition, an AGV is not a mobile robot because it lacks autonomy and the freedom to traverse a terrain (it is basically a single-degree-of-freedom moving platform along a built-in guide path). Similarly, "teleoperators," used in the nuclear industry for decades, are not mobile robots for the same reason: a human operator has full control over the vehicle. A teleoperator looks like a mobile robot because it has a chassis and a manipulator arm on top of it, but its on-board computer is programmed to follow the remote operator's commands. An example of a real mobile robot is the four-wheel Stanford Cart built in the late seventies.[1] This relatively simple robot, as well as some advanced ones, including an intelligent robotic vehicle recently developed for Lunar/Martian robotic missions, are described in the text to follow.

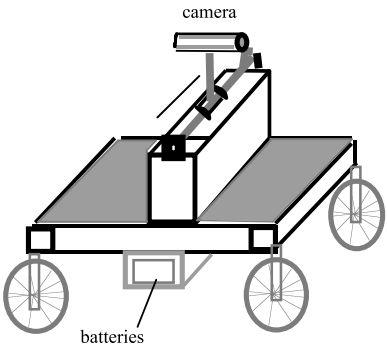

FIGURE 26.2 The Stanford Cart.

26.2.2 Stanford Cart

The cart was developed at the Stanford Artificial Intelligence Laboratory as a research setup for Ph.D. students (Figure 26.2). The robot was equipped with an on-board TV system and a computer dedicated to image processing and driving the vehicle through obstacle-cluttered spaces. The system gained its knowledge entirely from images. Objects were located in three dimensions, and a model of the environment was built with information gained while the vehicle was traversing a terrain. The system was unreliable for long runs and very slow (1 m in 10 to 15 min).

The operation would start at a certain point on a flat horizontal surface (flat floor) cluttered with obstacles. The camera was mounted on a sliding unit (50-cm track on top of the chassis) so that it was able to move sideways while keeping the line-of-sight forward. Such sidewise movements allowed the collection of several images of the same scene with a fixed lateral offset. By correlating those images the control system was able to identify locations of obstacles in the camera's field of vision. Control was simplified because these images were collected while the cart was inactive. After identifying the location of obstacles as simple fuzzy ellipsoids projected on the floor surface, the vehicle itself was modeled as a fuzzy ellipsoid projected on the same surface.

Based on the environment model a Path Planner was used to determine the shortest possible path to the goal-point. This program was capable of finding the path that was either a straight segment between the end and initial points, or a set of tangential segments and arcs along the ellipses (Figure 26.3). To simplify the algorithm, the ellipses were actually approximated by circles.

The navigation module was very primitive because the chart motor control lacked feedback. Thus, the vehicle was moved roughly in a certain direction by activating, driving, and steering motors for a brief time. After moving the vehicle for about 1 m, the whole procedure was repeated.

Although the whole process was extremely slow (roughly 4 to 6 m/h), and vehicle control very primitive, this was one of the first platforms that had all features needed for a robot to be regarded as a real mobile robot. It was autonomous and adaptable to environmental variations.

26.2.3 Intelligent Vehicle for Lunar/Martian Robotic Missions

In contrast to the Stanford Cart built as a students' experimental setup in the late 1970s, the intelligent robotic vehicle system (IRVS) was developed by the UA/NASA Space Engineering Research Center in the early 1990s.[2] This robot was developed to facilitate *in situ* exploration missions on the lunar/Martian surface. The system was designed to determine (1) site topography using two high-resolution CCD cameras and stereo-photogrammetry techniques; (2) surface mineral composition using two spectrometers, an oven soil heater, and a gas analyzer; and (3) regolith depths using sonar sounders. The primary goal of such missions was to provide accurate information that incorporates *in situ* resource utilization on the suitability of a site to become a lunar/Martian outpost. Such a lunar base would be built using locally available construction materials (rocks and

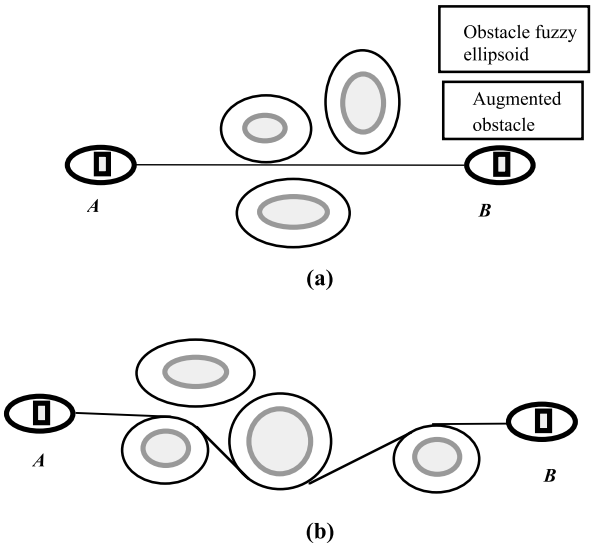

FIGURE 26.3 Path Planning results for two distinct scenarios: (a) a straight line segment exists between the initial and final point, ***A*** and ***B***; and (b) a path consists of a set of straight segments tangential to augmented obstacles, and arcs along the obstacle boundaries that are optimal in terms of its length.

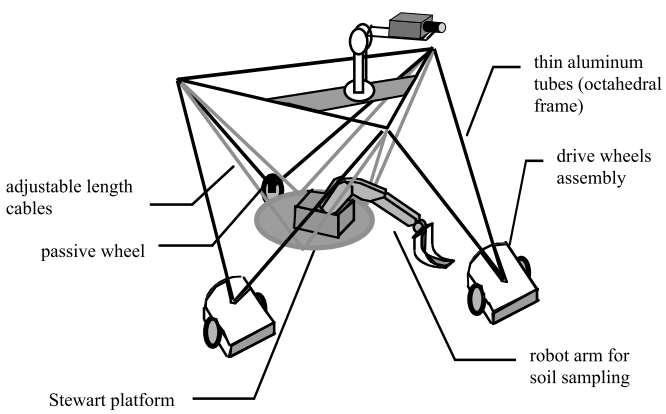

FIGURE 26.4 IRVS mobile robot.

minerals). The base would allow building plants for the production of oxygen and hydrogen for rocket fuel, helium for nuclear energy, and some metals. These materials would be used for building space stations with a cost far lower than the cost of transporting them from Earth.

The IRVS consists of a mobile platform, a manipulator arm, and a set of mission sensors. The most important requirement for the platform is exceptionally high payload-to-mass ratio. This was achieved by using a Stewart platform system developed by the U.S. National Institute of Standards and Technology (Figure 26.4). The structure consists of (1) an octahedral frame constructed of thin walled aluminum tubing, (2) three wheel assemblies (two of them have speed/skid steering control, while the third is a single free wheel), and (3) a work platform suspended by six cables arranged as a Stewart platform. The system is equipped with two high-resolution cameras with power zoom, auto iris, and focus capabilities mounted on a pan/tilt unit at the top of the octahedral frame. Ultrasonic ranging sensors were added for detects objects within a range of 0.2 to 12 m with a field of view of 6°. The system is also equipped with roll-and-pitch sensors that are used for controlling the six cables so that the work platform is always horizontal.

The IRVS control system is nontraditional, i.e., it is not based on sensing, planning, and executing control levels. It consists of a number of behavior programs organized in control levels: *organization*, *coordination,* and *execution*. The organization level consists of four behavior programs: (1) *site-navigator*, (2) *alternative sample collection point* (SCP) *selector*, (3) SCP *recorder*, and (4) SCP *organizer.*

The site-navigator uses a potential field method to calculate the vehicle's trajectory to the next SCP based on vision and range measurements. The alternative SCP selector picks an alternative SCP when a scheduled SCP cannot be reached due to obstacles/craters. The SCP recorder marks the points already visited so that the vehicle cannot sample a SCP twice. The SCP organizer generates a sequence of manipulator and instrument deployment tasks when the robot arrives at a SCP.

The coordination level contains *task-dispatcher* and *behavior arbitrator* programs. The task-dispatcher program analyzes the tasks submitted from the organization level, and activates the behaviors (tasks at the execution level) needed for successful completion of the task's requirements. It also implements a set of failure procedures when a given task cannot be executed because of possible failure (unstable vehicle, etc.). The behavior arbitrator assigns priorities to behaviors so that only the highest-priority behavior will be executed when two or more are simultaneously activated.

Execution level behaviors include the following tasks: obstacle-avoider, open-terrain explorer, etc. Obstacle avoiders are activated when an ultrasonic sensor measurement indicates the presence of an obstacle. Then, the site-navigator behavior is immediately suppressed due to its lower priority than that of the obstacle avoider. The purpose of the open-terrain explorer is to monitor obstacles in an open terrain situation and prevent the vehicle from becoming trapped among obstacles.

Clearly, IRVS control architecture is similar to that of a multitasking real-time kernel. Control is divided over a large number of tasks (called behaviors). The tasks are activated from a control kernel so that the highest-priority one will run first. The control algorithm implemented within a task (behavior) is usually simple and easy to test. The interdependencies among the control laws are implemented within the task's intercommunication network. Message envelopes, circular buffers, semaphores, sockets, and other communication means are used for this purpose. Such control architecture has "fine-granularity" so that elementary control tasks are simple. Still, the overall control architecture is very complex and difficult for theoretical analysis.

26.2.4 Mobile Robots — Nonholonomic Systems

The Stanford Cart and IRVS are just two examples of mobile robots. From these examples we see that mobile platforms can differ in many aspects including geometry, number of wheels, frame structure, etc. From a mechanical point of view there is a common feature to all systems: they are nonholonomic systems. In this section we explain exactly what that means.

Recall that the dynamic model of a manipulator with n degrees of freedom is described by

$$H(q)\ddot{q} + h(q,\dot{q}) = \tau - J^T(q)f \tag{26.1}$$

where $H(q)$ is the $n \times n$ inertia matrix; $h(q,\dot{q})$ is the n-vector due to gravity, centrifugal, and Coriolis forces; τ is the k-dimensional input vector (note that not all joints are necessarily equipped with actuators); $J(q)$ is a $m \times n$ Jacobian matrix; and f is the m vector of constraint forces. The constraint equation generally has the form

$$C(q,\dot{q}) = 0 \tag{26.2}$$

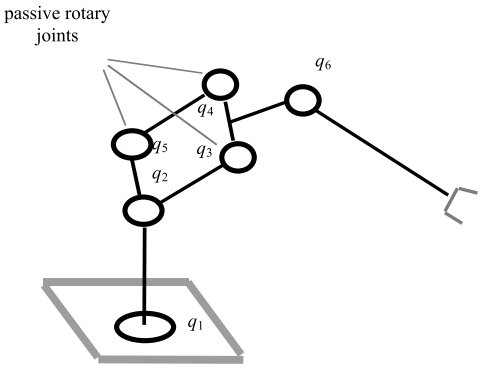

FIGURE 26.5 A manipulator with a closed-loop chain within its structure.

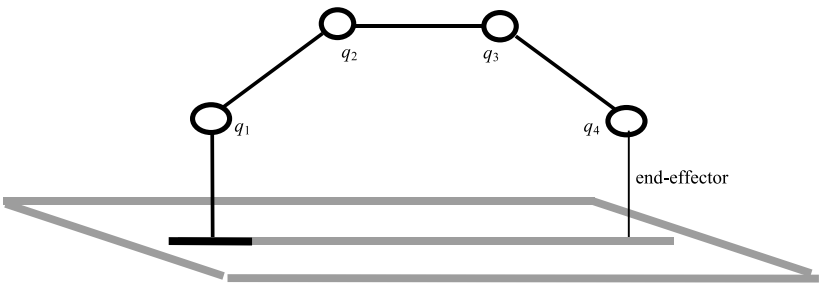

FIGURE 26.6 A manipulator in contact with the environment.

where C is an m vector. Note that the constraint Equation (26.2) involves both the generalized coordinates and its derivatives. In other words, the constraints may have their origins in the system's geometry and/or kinematics.

A typical system with geometric constraints is the robot shown in Figure 26.5. It has six joints (generalized coordinates), but only three degrees of freedom. Assuming that the closed loop chain ABCD is a parallelogram (Figure 26.5), the constraint equations are

$$q_3 + q_2 - \pi = 0$$

$$q_4 - q_2 = 0$$

$$q_5 + q_2 - \pi = 0$$

In this case the constraint equations have form $C_i(q) = 0$. Such constraints, or those that can be integrated into this form, are called *holonomic constraints*.

Another example is a four-degrees-of-freedom manipulator in contact with the bottom surface with an end-effector normal to the surface (Figure 26.6). Assuming that the link lengths are equal we obtain the following constraints:

$$q_1 - q_4 = 0$$

$$q_2 - q_3 = 0$$

$$q_1 + q_2 + q_3 + q_4 - 3\pi = 0$$

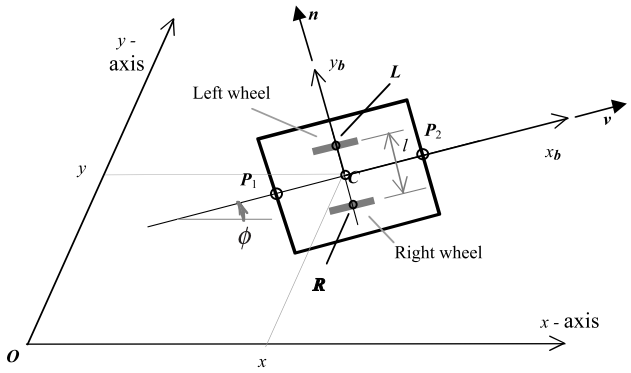

FIGURE 26.7 A simple mobile platform.

A typical system with both holonomic and nonholonomic constraints is a two-wheel platform supported by two additional free wheels in points $\boldsymbol{P}_1$ and $\boldsymbol{P}_2$ (Figure 26.7). Because the vehicle consists of three rigid bodies (a chassis and two wheels), we can select the following five generalized coordinates: x and y coordinates of the central point $\boldsymbol{C}$; an angle ϕ between the longitudinal axis of the chassis (x_b) and the x-axis of the reference frame; and θ_L and θ_R, the angular displacements of the left and right wheel, respectively. We assume that the wheels are independently driven and parallel to each other. The distance between the wheels is l.

The constraint equations can be derived from the fact that the vehicle velocity vector $\boldsymbol{v}$ is always along the axis x_b. In other words, the lateral component of the velocity vector (the one that is normal to the wheels) is zero. From Figure 26.7 we observe that the unit vector along x_b is $\mathbf{x}_b = (\cos\phi \sin\phi)^T$, while the vector normal to direction of motion is

$$\mathbf{x}_b = (\cos\phi \quad \sin\phi)^T$$

Because $\mathbf{v} = (\dot{x}, \ \dot{y})^T$, and $\mathbf{v}\cdot\mathbf{n} = 0$, we obtain the first constraint equation:

$$\dot{y}\cos\phi - \dot{x}\sin\phi = 0 \tag{26.3}$$

The other two constraint equations are obtained from the condition that the wheels roll, but do not slip, over the ground surface:

$$v_R = r\,\dot{\theta}_R$$

$$v_L = r\,\dot{\theta}_L$$

where v_R (v_L) is the velocity of the platform at the points $\boldsymbol{R}$ ($\boldsymbol{L}$) in Figure 26.7. Velocities $\dot{\theta}_R$ and $\dot{\theta}_L$ are angular velocities of the right- and left-hand side wheel. The velocity vector in either of these two points has two components: one due to the linear velocity of the chassis, and another due to the rotation of the chassis. The first component is easily obtained as

$$v = \dot{x}\cos\phi + \dot{y}\sin\phi \tag{26.4}$$

from

$$\dot{x} = v\cos\phi \tag{26.5}$$

$$\dot{y} = v\sin\phi \tag{26.6}$$

By multiplying Equation (26.5) by $\cos\phi$ and Equation (26.6) by $\sin\phi$, we easily get Equation (26.4). The second component of the velocity of the platform at the point $\boldsymbol{R}$ is

$$v_R = \frac{l}{2}\dot{\phi}$$

At the point $\boldsymbol{L}$ the velocity has the same magnitude, but the opposite sign

$$v_L = \frac{l}{2}\dot{\phi}$$

Now, we get the constraint equations for the wheels:

$$\dot{x}\cos\phi + \dot{y}\sin\phi + \frac{l}{2}\dot{\phi} = r\dot{\theta}_R \tag{26.7}$$

$$\dot{x}\cos\phi + \dot{y}\sin\phi - \frac{l}{2}\dot{\phi} = r\dot{\theta}_L \tag{26.8}$$

The obtained set of constraint equations can be easily converted into the matrix form Equation (26.2). Because the generalized coordinate vector has the form

$$\mathbf{q} = (x, y, \phi, \theta_R, \theta_L)^T$$

the constraint Equations (26.3), (26.7), and (26.8) can be presented in the matrix form

$$\begin{bmatrix} \sin\phi & -\cos\phi & 0 & 0 & 0 \\ -\cos\phi & -\sin\phi & l/2 & 0 & r \\ -\cos\phi & -\sin\phi & -l/2 & r & 0 \end{bmatrix} \dot{\mathbf{q}} = \mathbf{0} \tag{26.9}$$

This is a very characteristic form for nonholonomic constraints: $C(q, \dot{q}) = R(q)\dot{q} = 0$, with

$$R(q) = \begin{bmatrix} \sin\phi & -\cos\phi & 0 & 0 & 0 \\ -\cos\phi & -\sin\phi & l/2 & 0 & r \\ -\cos\phi & -\sin\phi & -l/2 & r & 0 \end{bmatrix}$$

In our case the matrix $R(q)$ is a 3×5 matrix. We also note that there are five generalized coordinates, and three constraint equations. This means that there are two dynamic equations to be written to complete the system (that is, to derive the full dynamic model of the system). Let us now return to the constraint equations. The question is, How many constraint equations are nonholonomic out of the three listed above? The general solution is based on the properties of matrix R, but such a solution is rather complicated (readers who are interested in this topic can find more information in Campion et al.[3]). Instead, we can come to the same conclusion by observing that there is a holonomic equation (constraint) hidden among the three constraint equations given above. To obtain this equation, we subtract Equation (26.8) from Equation (26.7):

$$l\dot{\phi} = r(\dot{\theta}_R - \dot{\theta}_L) \tag{26.10}$$

We can now integrate this equation over time and obtain

$$l\phi = r(\theta_R - \theta_L) + const. \tag{26.11}$$

where *const.* is a constant that depends on initial conditions (angles). This equation can be easily derived straight from the geometry of the system. Because there is no velocity-dependent term in this constraint equation, it is a holonomic one. The set of constraints now becomes

$$\begin{aligned} \dot{x}\cos\phi + \dot{y}\sin\phi + (l/2)\dot{\phi} &= r\dot{\theta}_R \\ \dot{y}\cos\phi - \dot{x}\sin\phi &= 0 \\ l\phi - r(\theta_R - \theta_L) &= 0 \end{aligned} \tag{26.12}$$

In conclusion, the mobile platform shown in Figure 26.7 has one holonomic and two nonholonomic constraints.

26.3 Dynamics of Mobile Robots

Although there has been a vast amount of research effort on modeling open and closed kinematic chains (manipulators), study of systems that include both the mobile platforms and manipulators mounted on top of them is very limited. The dynamic equations of such systems are far more complicated than those of simple manipulators. The first noticeable difference is in the state vector. It is common with manipulators to select joint coordinates and velocities as components of a state vector, but with mobile platforms there is no such simple clear rule. We recall (Figure 26.7) that the coordinates describing the platform position and orientation are x, y, ϕ, θ_R, θ_L. These coordinates are often referred to as "generalized coordinates." The state vector contains these five coordinates and their time-derivatives. The total number of state coordinates is thus ten. On the other hand, the vehicle in Figure 26.7 has only two degrees of freedom (from any position it can only advance for a vector $\Delta\boldsymbol{r}$ along its longitudinal axis, and rotate by an angle $\Delta\phi$ about its vertical rotation). Thus, only two equations are sufficient to describe the system dynamics. These two equations plus the three constraint equations derived in the previous paragraph constitute the mathematical model of the system.

The dynamic equations can be derived from Newton–Euler's formalism, or Lagrange equations, etc. Let us illustrate the derivation of the equations for the vehicle shown in Figure 26.7 using Newton's equations. This method relies on the system's forces and geometry. The forces that act on the chassis are imposed by the torques about the wheel axes (Figure 26.8).

The relationship between the force and the torque is

$$F_R r + I_W \ddot{\theta}_R = \tau_R \tag{26.13}$$

for the right-hand side wheel, and

$$F_L r + I_W \ddot{\theta}_L = \tau_L \tag{26.14}$$

for the left wheel. Here, I_W is the inertia of the wheel, while $\ddot{\theta}_L$ and $\ddot{\theta}_R$ are angular accelerations of the corresponding wheels. The forces $\boldsymbol{F}_R$ and $\boldsymbol{F}_L$ act on the vehicle at points R and L along the longitudinal axis $\boldsymbol{x}_b$. In general, they have different magnitudes, but their vectors are always parallel to each other. They may also have opposite signs, thus turning the chassis about the vertical axis.

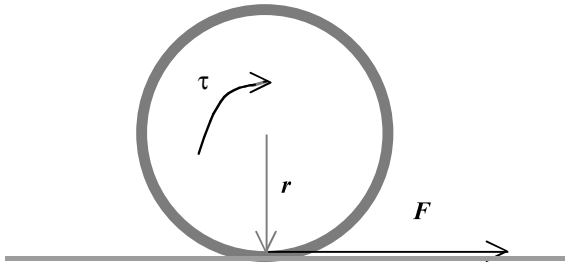

FIGURE 26.8 Wheel force and torque.

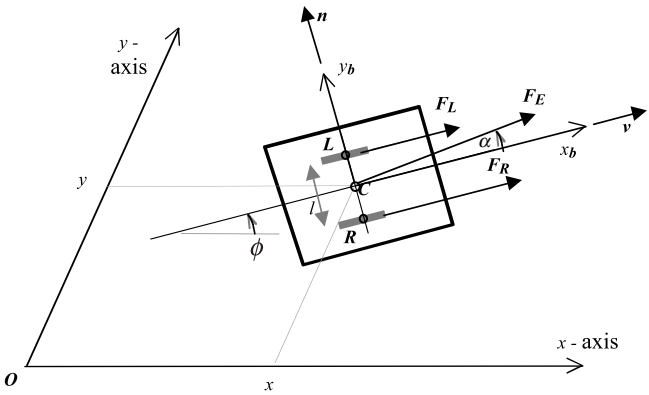

FIGURE 26.9 Forces acting on the mobile platform.

For the sake of generality, let us assume that an external force $\boldsymbol{F}_{\mathrm{E}}$ acts on the chassis at point C in addition to the forces $\boldsymbol{F}_{\mathrm{R}}$ and $\boldsymbol{F}_{\mathrm{L}}$.

Figure 26.9 shows that the total force along the axis x_b is

$$F_{x_b} = F_R + F_L + F_E \cos\alpha$$

while the force along the y_{b} axis is

$$F_{y_b} = F_E \sin\alpha$$

This yields the components along the x and y axes of the reference frame:

$$\begin{aligned} F_x &= (F_R + F_L + F_E \cos\alpha)\cos\phi - (F_E \sin\alpha)\sin\phi \\ F_y &= (F_R + F_L + F_E \cos\alpha)\sin\phi + (F_E \sin\alpha)\cos\phi \end{aligned} \tag{26.15}$$

Finally, we obtain the equations of motion

$$\begin{aligned} F_x &= m\ddot{x} \\ F_y &= m\ddot{y} \end{aligned} \tag{26.16}$$

where m is the mass of the vehicle (chassis + wheels). The moment equation is rather simple:

$$\frac{l}{2}(F_R - F_L) = I\ddot{\phi} \tag{26.17}$$

By combining Equations (26.15) and (26.16), and by grouping these two equations with Equations (26.13), (26.14), and (26.17), we obtain the dynamic model of the vehicle:

$$\begin{aligned} m\ddot{x} - (F_R + F_L + F_E\cos\alpha)\cos\phi + (F_E\sin\alpha)\sin\phi = 0 \\ m\ddot{y} - (F_R + F_L + F_E\cos\alpha)\sin\phi - (F_E\sin\alpha)\cos\phi = 0 \\ I\ddot{\phi} - \frac{l}{2}(F_R - F_L) = 0 \\ I_W\ddot{\theta}_R + F_R r = \tau_R \\ I_W\ddot{\theta}_L + F_L r = \tau_L \end{aligned} \tag{26.18}$$

The forces F_R and F_L are generated between the ground and the wheels. The external force has two components: one along the chassis, and another perpendicular to the chassis. Obviously, the latter does not contribute to motion and can have any value below a limit that would cause lateral sliding of the chassis. The external force can be generated by mechanical means (cable-pulling system), electromagnetic means (attraction or repulsion force in a magnetic or electrostatic field), chemical reaction force (by the action of jets), etc. For the sake of simplicity, let us assume that the external force component acting along the vehicle is zero so that only a lateral component exists. In this case, the angle α equals 90°, and we have the following equations:

$$\begin{aligned} m\ddot{x} - (F_R + F_L)\cos\phi + F_E\sin\phi = 0 \\ m\ddot{y} - (F_R + F_L)\sin\phi - F_E\cos\phi = 0 \\ I\ddot{\phi} - \frac{l}{2}(F_R - F_L) = 0 \\ I_W\ddot{\theta}_R + F_R r = \tau_R \\ I_W\ddot{\theta}_L + F_L r = \tau_L \end{aligned} \tag{26.19}$$

The dynamic model Equation (26.19) includes constrained forces F_R and F_L, and F_E. The model Equation (26.19) and the constraint Equations (26.12) describe the dynamic behavior of the system. The matrix form of the constraint equations derived in the previous section is

$$C(q,\dot{q}) = R(q)\dot{q} = 0 \tag{26.20}$$

Note that the matrix form of Equation (26.19) has the form equal to the one that holds for the manipulators in Equation (26.1). It can be easily shown that Equation (26.19) can be presented in the form

$$H(q)\ddot{q} + h(q,\dot{q}) = T(q)\boldsymbol{\tau} - R^T(q)\boldsymbol{f} \tag{26.21}$$

where q is the vector of generalized coordinates:

$$q = [x\ y\ \phi\ q_R\ q_L]^T$$

$\boldsymbol{f}$ is a vector of constrained forces $\boldsymbol{f} = (F_R, F_L, F_E)^T$, and $\boldsymbol{\tau} = (\tau_R, \tau_L)^T$ is the driving torque vector. The matrix T is called the "input transformation matrix." Comparing Equations (26.20) and (26.21) we see that $H(q) = \text{diag}(m, m, I, I_W, I_W)$. This means that the inertia matrix is a 5×5 diagonal matrix. This matrix is always symmetric, but not necessarily diagonal. Any offset in the center of mass would actually bring nondiagonal elements into existence. The matrix h is zero, but in general it has velocity-dependent terms. These terms have only quadratic forms (either square or the product of two velocities). Matrix T is a 5×2 matrix with the elements:

$$T(q) = \begin{bmatrix} 0 & 0 \\ 0 & 0 \\ 0 & 0 \\ 1 & 0 \\ 0 & 1 \end{bmatrix}$$

Finally, matrix R has the form

$$R(q) = \begin{bmatrix} \sin\phi & -\cos\phi & 0 & 0 & 0 \\ -\cos\phi & -\sin\phi & l/2 & 0 & r \\ -\cos\phi & -\sin\phi & -l/2 & r & 0 \end{bmatrix}$$

which is equal to that derived in the previously (see Equation 26.9).

$R(q)\dot{q} = 0$ shows that a certain relationship exists between the components of the vector $\dot{q}$. Indeed, each component of $\dot{q}$ can be expressed in terms of $\dot{\theta}_R$ and $\dot{\theta}_L$. For example, $\dot{x} = v\cos\varphi$, where v is the velocity of the chassis equal to

$$v = \frac{1}{2}(v_R + v_L)$$

$$= \frac{1}{2}(r\dot{\theta}_R + r\dot{\theta}_L)$$

yields

$$\dot{x} = \frac{r}{2}(\cos\phi)(\dot{\theta}_R + \dot{\theta}_L) \tag{26.22}$$

Similarly, we get

$$\dot{y} = \frac{r}{2}(\sin\phi)(\dot{\theta}_R + \dot{\theta}_L) \tag{26.23}$$

Finally, Equation (26.10) yields

$$\dot{\phi} = \frac{r}{l}(\dot{\theta}_R - \dot{\theta}_L) \tag{26.24}$$

From Equations (26.22 to 26.24) we obtain

$$\begin{bmatrix} \dot{x} \\ \dot{y} \\ \dot{\phi} \\ \dot{\theta}_R \\ \dot{\theta}_L \end{bmatrix} = \begin{bmatrix} \frac{r}{2}\cos\phi & \frac{r}{2}\cos\phi \\ \frac{r}{2}\sin\phi & \frac{r}{2}\sin\phi \\ \frac{r}{l} & -\frac{r}{l} \\ 1 & 0 \\ 0 & 1 \end{bmatrix} \begin{bmatrix} \dot{\theta}_R \\ \dot{\theta}_L \end{bmatrix} \tag{26.25}$$

We now observe that only two components of the vector $\dot{q}$ determine all others. These two components are the velocities of the wheels. Equation (26.25) in general has the form

$$\dot{q} = S(q)v \tag{26.26}$$

where $\dot{q}_0$ is a subvector of $\dot{q}$. There is an important relationship between R and S that can be easily derived by substituting Equation (26.26) into $R(q)\dot{q} = 0$:

$$RS = S^{\mathrm{T}}R^{\mathrm{T}} \tag{26.27}$$

This property is necessary to obtain the state-space model of the mobile robot. To derive this model we first have to find the acceleration vector $\ddot{q}$ by differentiating Equation (26.26) with respect to time:

$$\ddot{q} = S(q)\dot{v} + \dot{S}(q)v \tag{26.28}$$

Then we substitute the acceleration vector Equation (26.28) into the dynamic model Equation (26.21), and obtain the model in a simple form:

$$\bar{H}\dot{v} + \bar{h} = S^T T(q)\boldsymbol{\tau} \tag{26.29}$$

where $\bar{H} = S^T H S$, and $\bar{h} = S^T H \dot{S} v + S^T h$.

A number of important conclusions are based on the form of the model Equation (26.29). First, the time derivative of the vector v contains accelerations of the "core" variables: wheel coordinates. Matrix $\bar{H} = S^T H S$ depends on coordinates, and represents an inertia matrix as seen from the "wheels." Vector $\bar{h}$ depends on system coordinates and velocities. The dimension of the matrices in the model Equation (26.29) equals the number of core coordinates (in our example, the dimension of the matrix $\bar{H}$ is 2×2. This model is very useful for system simulation and control.

26.4 Control of Mobile Robots

A variety of control systems with mobile robots are currently in use. The simplest control systems were developed for so-called "teleoperators" more than 20 years ago. The teleoperators are remotely driven mobile platforms equipped with a manipulator aimed at performing various tasks in nuclear and hazardous environments. Radio or cable link is used to connect the teleoperator with the control

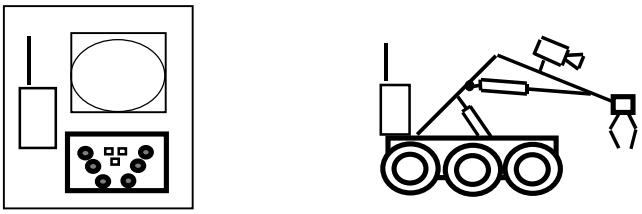

FIGURE 26.10 Teleoperator.

station (Figure 26.10). The control station consists of a TV monitor, and a control panel with joysticks and pushbutton commands. Bi-directional radio links allow simultaneous transmission of

1. Commands from the control panel (CP) to the robot actuators (those that drive the chassis, and control the configuration of the arm)
2. Robot-mounted camera signal to be shown on the TV monitor
3. Voice signal in both directions

Let us denote the control signals from the CP's joysticks as u_c, and assume that the chassis is of the type shown in Figure 26.9. In most applications the power drivers to the chassis motors are current-mode drivers, that is, motor current is proportional to the input signal. Since the electromagnetic torque produced by the motor current is proportional to the current, we can simply express the whole control system as

$$\begin{aligned} \bar{H}\dot{v} + \bar{h} &= S^T T(q)\boldsymbol{\tau} \\ \boldsymbol{\tau} + \boldsymbol{\tau}_f &= k_t u_c \end{aligned} \tag{26.30}$$

where the first equation is Equation (26.29). The friction torque in the gear train and between the wheels and the ground (tracks) is modeled by τ_f. The constant that relates torque and the input signal is denoted as k_t. Such control is very imprecise because of the significant amount of friction in the drive train that is not compensated by the control system. Typically, the vehicle poorly follows the commands especially in transition from a static to a dynamic state (motion). There is no way that small and precise increments in position/orientation can be precisely commanded. Still, such control has theoretical significance, and we will elaborate in more details how a torque control scheme can be developed. Let us assume that the force between the wheel and the chassis (F_R and F_L in Equation 26.19) is measured by strain gauges or force sensors. In such cases, control can be formulated as a PI control on the force-error signal:

$$\begin{aligned} \tau_R &= k_F \frac{1}{r}(F_{Rd} - F_R) + k_{FI}\int (F_{Rd} - F_R)dt \\ \tau_L &= k_F \frac{1}{r}(F_{Ld} - F_L) + k_{FI}\int (F_{Ld} - F_L)dt \end{aligned} \tag{26.31}$$

By tuning the gains k_F and k_{FI} the measured force will more or less follow the desired one (F_{Rd} and F_{Ld}). The error becomes smaller with higher gains, but stability will be affected at high gains due to the presence of noise. Assuming the prefect control of forces F_R and F_L, we obtain a model of the mobile platform as follows:

$$m\ddot{x} - (F_R + F_L)\cos\phi = 0$$

$$m\ddot{y} - (F_R + F_L)\sin\phi = 0$$

$$I\ddot{\phi} - \frac{l}{2}(F_R - F_L) = 0$$

Here we can assume that F_R and F_L are control inputs. Or, alternatively, we can introduce the following control inputs

$$u_1 = F_R + F_L$$

$$u_2 = F_R - F_L$$

so that the model becomes

$$\begin{aligned} m\ddot{x} &= u_1 \cos\phi \\ m\ddot{y} &= u_1 \sin\phi \\ I\ddot{\phi} &= \frac{l}{2} u_2 \end{aligned} \tag{26.32}$$

This is a second-order dynamic model of the platform assuming that all damping and friction forces are compensated by the use of force-feedback. Although relatively simple, this model exhibits nonholonomic properties. This can be illustrated as follows: assume the system is in the state (x, y, ϕ) = (0,0,0). The model of the chassis in this position and orientation becomes

$$\begin{aligned} m\ddot{x} &= u_1 \\ m\ddot{y} &= 0 \\ I\ddot{\phi} &= \frac{l}{2} u_2 \end{aligned}$$

indicating that the system is impossible to control in the y-direction from the given state. Or, in other words, the platform behaves as a singular system in the y-direction.

This system Equation (26.32), as well as the original system Equation (26.19), has very important properties that are elaborated by Zheng.[4]

1. The system (Equations 26.32 and 26.19) is a nonholonomic controllable system.
2. The system (Equations 26.32 and 26.19) cannot be made asymptotically stable by a smooth-state feedback.

The term "controllable" refers to the following: if a system can be transferred from any state to any other state by finite control signals in a finite time, it is a controllable system. With linear systems it would automatically imply the existence of smooth feedback that guarantees asymptotic stability. This does not hold for nonlinear systems as stated by the second property.

The developed control scheme is not used in practice. The control scheme based on local-velocity feedback loops is used much more often. A tachometer exists on every wheel to measure the speed of rotation of the wheel with such vehicles. The right-hand side wheel dynamics and control are then described by

$$\begin{aligned} F_R r + I_W \ddot{\theta}_R &= \tau_R \\ \tau_R + \tau_f &= k_v(\dot{\theta}_{Rd} - \dot{\theta}_R) \end{aligned} \tag{26.33}$$

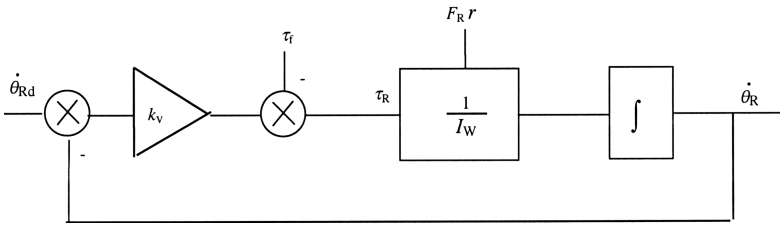

FIGURE 26.11 Control diagram based (Equation 26.33).

where k_v is the velocity feedback constant. The same model holds for the left wheel (the subscript R should be replaced by L). The control diagram based Equation (26.33) is shown in Figure 26.11.

Note that in this control scheme the friction torque and the torque due to the presence of driving force F_R act as a disturbance to the system. The goal of such control is to maintain the wheel velocity as close as possible to the desired velocity. The feedback gain k_v is usually tuned to a large value so that the velocity error

$$e = \dot{\theta}_{Rd} - \dot{\theta}_R$$

is small, while control is still stable. Here, the joystick control output equals

$$u_c = \dot{\theta}_{Rd}$$

Obviously, fine commands (small joystick increments) will be amplified by the gain k_v so that the wheel driver will be able to produce motion. This crucial and fine motion of the chassis is required from any static position. Assume, for example, that the vehicle is at rest and that the rotation by an angle ϕ of only one degree is required. This is usually impossible by the direct control scheme, and becomes possible with the velocity control loop. This is clear from Equation (26.20):

$$\dot{\phi} = \frac{r}{l}(\dot{\theta}_R - \dot{\theta}_L)$$

which shows that the better speed control in the wheels, the better overall turning ability of the chassis.

Having high-velocity gains in wheel controllers has another important implication on the behavior of the overall system — it simplifies the system's behavior if we assume that the real wheel velocity is equal to the desired (commanded) one. In this case, the above equation becomes

$$\dot{\phi} = \frac{r}{l}(u_R - u_L) \tag{26.34}$$

where u_R and u_L are left- and right-wheel control inputs. From (Equations 26.22 and 26.23) we obtain:

$$\dot{x} = \frac{r}{2}(\cos\phi)(u_R + u_L) \tag{26.35}$$

and

$$\dot{y} = \frac{r}{2}(\sin\phi)(u_R + u_L) \tag{26.36}$$

The last three equations constitute the new model of the system. We can also introduce the control signals u_1 and u_2 instead of u_R and u_L such that

$$u_1 = u_R + u_L$$

$$u_2 = u_R - u_L$$

Now, the system model becomes

$$\begin{aligned} \dot{x} &= \frac{r}{2} u_1 \cos\phi \\ \dot{y} &= \frac{r}{2} u_1 \sin\phi \\ \dot{\phi} &= \frac{r}{l} u_2 \end{aligned} \tag{26.37}$$

We see that this model has a very similar form to Equation (26.32). The difference is in the order of the model: Equation (26.37) is a first-order model, while Equation (26.32) is a second-order one. Properties one and two listed above for the model Equation (26.32) hold also for model Equation (26.37). Another interesting property that also holds for Equations (26.37 and 26.32) is that the system is not full-state linearizable via static feedback loop. This means that no such (nonlinear) feedback loop can transform the system into a linear one. We recall that with manipulator models it is possible to introduce a nonlinear feedback loop that can fully linearize the system. Let us repeat, for clarity — if the dynamic model of a manpulator is

$$H\ddot{q} + h = u$$

then the nonlinear control

$$u = H(\ddot{q}^0 + k_v(\dot{q}^0 - \dot{q}) + k_p(q^0 - q)) + h$$

generates the error equation

$$(\ddot{q}^0 - \ddot{q}) + k_v(\dot{q}^0 - \dot{q}) + k_p(q^0 - q) = 0$$

so that the overall system becomes linear. As stated above, this is impossible with the models (Equations 26.32 and 26.37).

From the discussion above it is clear that no simple linear control can stabilize the system Equation (26.37). A number of different nonlinear control laws have been proposed in the literature, for example, tracking control, path following, stabilization about a desired posture, etc.

Let us illustrate control strategy in an example of tracking control. For example, tracking control is based on the reference model (vehicle)

$$\begin{aligned} \dot{x}_r &= \frac{r}{2} u_{1r} \cos\phi_r \\ \dot{y}_r &= \frac{r}{2} u_{1r} \sin\phi_r \\ \dot{\phi}_r &= \frac{r}{l} u_{2r} \end{aligned}$$

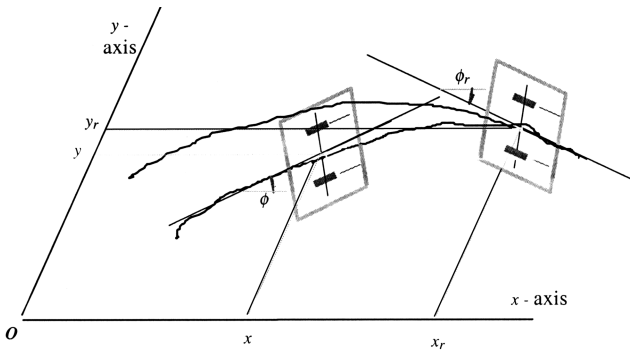

FIGURE 26.12 Tracking control illustration.

that has bounded control inputs that do not tend to zero when t approaches infinity. The control goal is to achieve zero asymptotic error in state difference (Δx, Δy, $\Delta\phi$) between the real and the reference model when $t \rightarrow$ infinity.

The control

$$u_1 = u_{1r}\cos(\phi_r - \phi) + \frac{2k_1}{r}e_1$$

$$u_2 = u_{2r} + \frac{k_2 l}{2}u_{1r}\frac{\sin(\phi_r - \phi)}{\phi_r - \phi}e_2 + \frac{k_3 l}{r}(\phi_r - \phi)$$

where

$$e_1 = (x_r - x)\cos\phi + (y_r - y)\sin\phi$$

$$e_2 = -(x_r - x)\sin\phi + (y_r - y)\cos\phi$$

and k_i are positive constants (i = 1, 2, 3).

It was shown[4] that this control globally asymptotically stabilizes the system so that the error in (Δx, Δy, $\Delta\phi$) tends to zero with time. As a consequence, the platform will follow the reference one and the error will tend toward zero with time. The proof is based on a suitable Liapunov function, which is nonincreasing along any system solution. An illustration of the tracking control is given in Figure 26.12.

Similar control laws have been developed for stabilization about a point and path-following problem. As a result, we see that the control problem is nonlinear and by no means a straightforward application of simple control theory.

There are many other practical issues related to the control of mobile robots. First is the sensorial system that can provide a good estimate of the platform position and orientation. Ultrasonic, infrared, laser-based, and camera-based sensors usually do this. Most of these sensors are used to detect a distance from an obstacle, and give information on the relative position of the vehicle with respect to the environment. Absolute coordinates are possible to get through GPS, which uses information on the geographic position of the robot obtained from a satellite by a radio link. One or more processors or microcontrollers process the sensor signals. The processors provide communication and control functions.

References

1. Moravec, P.H., The Stanford Cart and the CMU Rover, in *Autonomous Robot Vehicles,* Cox, I.J. and Wilfong, G.T., Eds., Springer-Verlag, New York, 1990, 407–419.
2. Wang F.-Y. and Lever, P.J.A., An intelligent robotic vehicle for lunar and Martian resource assessment, in *Recent Trends in Mobile Robots,* Zheng, Y.F., Ed., World Scientific, Singapore, 293–313.
3. Campion, G., d'Andrea-Novel, B., and Bastin, G., Controllability and state feedback stabilization of nonholonomic mechanical systems, in *Lecture Notes in Control and Information Science,* de Wit, C.C., Ed., Springer-Verlag, New York, 1991, 106–124.
4. Zheng, Y.F., *Recent Trends in Mobile Robots,* World Scientific, Singapore, 1993.